

# Can a Satellite Galaxy Merger Explain the Active Past of the Galactic Centre?

M. Lang<sup>1</sup>, K. Holley-Bockelmann<sup>1,2</sup>, T. Bogdanović<sup>3,4</sup>, P. Amaro-Seoane<sup>5,6</sup>, A. Sesana<sup>5</sup> & M. Sinha

<sup>1</sup>*Department of Physics and Astronomy, Vanderbilt University, Nashville, TN email: meagan.lang, manodeep.sinha@vanderbilt.edu*

<sup>2</sup>*Fisk University, Department of Physics, Nashville, TN email: k.holley@vanderbilt.edu*

<sup>3</sup>*Department of Astronomy, University of Maryland, College Park, MD 20742, e-mail: tamarab@astro.umd.edu*

<sup>4</sup>*Einstein Postdoctoral Fellow*

<sup>5</sup>*Max Planck Institut für Gravitationsphysik (Albert-Einstein-Institut), D-14476 Potsdam, Germany, email: pau.amaro-seoane, alberto.sesana@aei.mpg.de*

<sup>6</sup>*Institut de Ciències de l'Espai (CSIC-IEEC), Campus UAB, Torre C-5, parells, 2<sup>na</sup> planta, ES-08193, Bellaterra, Barcelona, Spain*

## ABSTRACT

Observations of the Galactic centre (GC) have accumulated a multitude of “forensic” evidence indicating that several million years ago the centre of the Milky Way galaxy was teeming with star formation and accretion-powered activity – this paints a rather different picture from the GC as we understand it today. We examine a possibility that this epoch of activity could have been triggered by the infall of a satellite galaxy into the Milky-Way which began at the redshift of  $z = 8$  and ended few million years ago with a merger of the Galactic supermassive black hole with an intermediate mass black hole brought in by the inspiralling satellite.

**Key words:** galaxies: interactions — Galaxy: centre — Galaxy: kinematics and dynamics — Galaxy: nucleus

## 1 INTRODUCTION

There is mounting observational evidence that the epoch that ended several million years ago was marked by an unusual level of activity in the Galactic centre (GC). This is remarkable given that at the current epoch, the GC is best characterized by the quiescent and underluminous nature of Sgr A\* (Genzel et al. 2010). The picture of the GC as a once powerful nucleus has begun to emerge from circumstantial observational evidence, most recently strengthened by a discovery of the “Fermi bubbles”, a pair of giant gamma-ray emitting bubbles that extend nearly 10 kpc north and south of the GC (Dobler et al. 2010; Su et al. 2010). Although there are alternative steady state models for forming the bubbles (Crocker et al. 2011), the well defined shock fronts at their edges suggest an abrupt origin. Current explanations include a past accretion event onto the supermassive black hole (SMBH; Su et al. 2010; Zubovas et al. 2011), AGN jets (Guo & Mathews 2011), a nuclear starburst (Su et al. 2010), and a sequence of star capture events in the last  $\sim 10$  Myr (Cheng et al. 2011). The period of increased gamma-ray activity is consistent with the finding that until several hundred years ago Sgr A\* was orders of magnitude more X-ray luminous than it is today, as indicated by the echo in the fluorescent Fe K line emission detected in the direction of the molecular clouds in the vicinity of Sgr A\* (Inui et al. 2009; Ponti et al. 2010; Terrier et al. 2010). Although we cannot be certain that the current quiescence of the GC is unusual, it appears clear that the GC experienced an active phase as recently as a few hundred years ago.

The GC is also a hotbed of star formation containing the three

most massive young star clusters in the Galaxy: the Central cluster, the Arches cluster, and the Quintuplet cluster (see Figer 2008, for a review). The three clusters are similar in many respects. Each cluster contains  $\sim 10^4 M_{\odot}$  in stars and has central stellar mass density that exceeds those measured in most globular clusters. While our current understanding of massive star and star cluster formation is incomplete, it is plausible that these clusters are all characterized by the star formation event within the past 2–7 Myr that resulted in the formation of more massive stars (above  $100 M_{\odot}$ ) than anywhere else in the Galaxy (Krabbe et al. 1995; Paumard et al. 2006). It is possible that the three clusters have a common origin and that they have formed as a consequence of a single event that triggered the flow of the copious amounts of gas into the central  $\sim 50$  pc in the Galaxy (though see Stolte et al. 2008, for a scenario in which the Arches cluster forms at the intersection of X1/X2 gas orbits in the inner Galaxy).

On even smaller scales, the existence of massive and young stars in the Central cluster, well within the central parsec, is especially puzzling given their close proximity to the central SMBH. Among those scenarios proposed are: in-situ formation (Bonnell & Rice 2008; Mapelli et al. 2012), in-spiral and consequent disruption of a dense stellar cluster with a central intermediate mass black hole (IMBH) (Merritt, Gualandris & Mikkola 2009), and binary disruption by massive perturbers (Perets & Gualandris 2010). A clue in favor of the in-situ formation is that most O and Wolf-Rayet type stars at the galactic center seem to inhabit one or more disc-like structures, pointing to their birth in a dense accretion disc (Bartko et al. 2010; Bonnell & Rice 2008; Mapelli et al. 2012). Star formation in

a gaseous disc also provides a natural explanation for the cuspy distribution of the young stars. In order for starforming clumps to withstand tidal forces in the inner parsec of the GC their densities need to be in excess of  $10^{11} \text{ cm}^{-3}$ , at least five orders of magnitude higher than the average density of molecular clouds in the GC (Figer et al. 2000). Such densities can only be achieved through highly compressive events (Figer 2008) and it is plausible that both the inflow of large amounts of gas into the GC and its shocking and compression have been caused by a common culprit. Both phenomena are found to arise as consequences of galactic mergers (Noguchi 1988; Barnes & Hernquist 1991, 1992, 1996; Mihos & Hernquist 1996; Hopkins & Quataert 2010) making this a possibility worth examining.

Further evidence that the MW has recently survived a dramatic event comes from the distribution of late-type stars in the GC. While the early-type stellar distribution appears to be cuspy (Genzel et al. 2003; Paumard et al. 2006; Buchholz et al. 2009; Do et al. 2009; Bartko et al. 2010), there seems to be a distinct lack of late-type stars. This evidence is based on number counts of spectroscopically identified late-type stars brighter than magnitude  $K = 15.5$  within the sub-parsec region about Sgr A\*. The best fits of the inner density profile for the late-type stellar population seem to favor power-laws with slopes of  $\gamma < 1$  and even allow the possibility of a core with  $\gamma < 0$ , with the stellar density decreasing toward the centre (Buchholz et al. 2009; Do et al. 2009; Bartko et al. 2010). At this stage, the evidence for a deficit of late-type stars is compelling, however there are still significant uncertainties in the density profile: the population of stars on which this inference has been made are luminous late-type giants that comprise only a small fraction of the underlying stellar density of the late-type population. Regardless of the precise slope, however, the distribution of the late-type population is contrasted by the steeply rising density distribution of early-type stars.

Possible mechanisms that could create a core in the distribution of late-type stars have been discussed by Merritt (2010) and include 1) stellar collisions that strip red giants of their envelopes such that they are under-luminous, 2) destruction of stars on orbits that pass close to the SMBH in a triaxial nucleus, 3) inhibited star formation near the SMBH at the time when the late-type population was formed, and 4) ejection of stars by a massive black hole binary. In light of the other evidence that points to a discrete event in the recent history of the GC, it is interesting to revisit the latter mechanism.

In giant elliptical galaxies, the existence of cores is often attributed to ejection of stars by an inspiralling binary SMBH (Merritt & Cruz 2001; Faber et al. 1997; Ferrarese et al. 2006; Milosavljević & Merritt 2001) and possibly due to gravitational wave recoil after binary coalescence (Boylan-Kolchin et al. 2004; Gualandris & Merritt 2008). The prediction of these models is that the central stellar mass deficit (traced by the stellar light) is proportional to the mass of the central black hole,  $M_{\text{def}} \propto M_{\bullet}$  (Graham 2004; Hopkins & Hernquist 2010). This correlation is interesting in view of the observed dichotomy between ellipticals with cores and those with the extra central light: core light deficit was found to correlate closely with  $M_{\bullet}$  and stellar velocity dispersion  $\sigma$ , in agreement with the theoretical predictions (Milosavljević & Merritt 2001; Gualandris & Merritt 2008), however, the extra light does not (Kormendy & Bender 2009). An explanation of these phenomena offered by Kormendy & Bender (2009) is that the extra light ellipticals were made in wet mergers with starbursts, where stars formed from gas leftover after the merger, while core ellipticals were created in dry mergers. In galax-

ies with excess light, the newly formed population of stars fills the core left in the distribution of the older population to form a steep cusp, thus giving rise to characteristic differences in the two stellar populations that may be mirrored in the MW GC.

Because studies of the light excess and deficit in elliptical galaxies focus on major mergers, the scenario seems less relevant for a disc-dominated system like the Milky Way, which may have never experienced a major merger (Gilmore et al. 2002). A minor merger of the SMBH with an IMBH however cannot be ruled out. The presence of an IMBH in the Galactic centre has been previously considered as a possible vehicle for delivery of young stars into the GC (Hansen & Milosavljević 2003), a mechanism for creation of hypervelocity stars (Baumgardt et al. 2006), and for the growth of the SMBH (Portegies Zwart et al. 2006). Indeed, the possibility that an IMBH with mass  $\lesssim 10^4 M_{\odot}$  is still lurking in the inner parsec of the GC cannot currently be totally excluded based on observations (Hansen & Milosavljević 2003; Genzel et al. 2010; Reid & Brunthaler 2004; Gualandris & Merritt 2009; Gualandris, Gillessen & Merritt 2010).

In light of the new observational evidence, which supports the notion that few to 10 Myr ago was a special period in the life of Sgr A\*, as indicated by the relatively recent episode of star formation and increased energy output, we revisit the possibility that a minor merger could have triggered this epoch of enhanced activity. We suggest that the cumulative observational evidence favors the minor merger hypothesis relative to the scenarios that propose a steady state evolution or passive relaxation of the GC region. We present a theoretical scenario for one such minor merger in § 2 and discuss the implications in § 3.

## 2 MILKY WAY – SATELLITE MERGER SCENARIO

Here we examine the viability of the following scenario: at high redshift, a primordial satellite galaxy with a central IMBH begins to merge with a young Milky Way. As the satellite sinks toward the GC under the influence of dynamical friction it is tidally stripped and its orbit gradually decays toward the Milky Way disc plane (Quinn & Goodman 1986; Callegari et al. 2011). The satellite perturbs previously stable gas clouds in the inner Milky Way disc, driving gas inflow (Noguchi 1988; Barnes & Hernquist 1991, 1996; Hopkins & Quataert 2010) and compressing the gas to densities exceeding those necessary for massive star formation near the GC (Mihos & Hernquist 1996; Hopkins & Quataert 2010). The satellite galaxy is expected to be largely disrupted by the time it reaches the GC, leaving the IMBH spiraling in a dense gaseous and stellar environment. In the context of this scenario we hypothesize that the IMBH reached the central parsec on the order of  $\sim 10$  Myr ago. A fraction of perturbed gas that did not form stars accretes onto the Milky Way’s SMBH (Hopkins & Quataert 2010), injecting massive amounts of energy into the surrounding medium and giving rise to the Fermi bubbles (Su et al. 2010; Zubovas et al. 2011). Once gravitationally bound, the IMBH-SMBH binary orbit tightens via three-body interactions with surrounding stellar background, scouring the old stellar population to form a central core (Merritt 2010). Finally, the binary coalesces after emitting copious gravitational radiation (Peters & Mathews 1963).

In the context of this hypothetical scenario we use the new GC observations to constrain the initial masses of the satellite and Milky Way galaxies ( $M_{\text{sat}}$  and  $M_{\text{MW}}$ ), the mass deficit in the late-type stellar population ( $M_{\text{def}}$ ), the IMBH mass ( $M_{\text{IMBH}}$ ), as well as the amount of gas inflow into the GC triggered by the inspiral of

the satellite galaxy. The properties of the satellite bound to reach the inner disc of the Milky Way and deliver its IMBH to the GC must satisfy several criteria: 1. it should be light enough not to disrupt the Galactic disc, 2. it should be sufficiently massive in order for the dynamical friction to operate efficiently and deliver it to the GC within a Hubble time, and 3. its potential well should be sufficiently deep to sustain tidal stripping by the Milky Way. We therefore focus on constraining the most plausible scenario given the current understanding of the processes involved.

Our approach is, out of necessity, semi-analytical in nature. While advanced cosmological *n*-body simulations are capable of modeling the accretion of a low-mass satellite galaxy onto cosmologically growing Milky Way halo, there are a number of physical processes important to our model that these simulations cannot capture. For example, we will capture the effect of the Milky Way disc, bulge and SMBH, and will account for the stabilizing effect of the IMBH within the satellite. In our model, we also include the critical effects of 3-body scattering and gravitational wave emission, both of which are beyond the reach of a cosmological *n*-body simulation.

## 2.1 Properties of the Progenitor Milky Way

Beginning the merger at high redshift is advantageous in three respects. First, at this early epoch, it is reasonable to assume that the proto-Milky Way was surrounded by primordial satellite galaxies capable of housing a central seed black hole (e.g., Ricotti & Gnedin 2005; Gnedin & Kravtsov 2006; Wise & Abel 2008; Micic et al. 2011). Second, at this stage in its growth, the Milky Way would have been smaller, less massive, and more gas-rich than it is today, thus decreasing the time required for the satellite to sink to the galactic centre via dynamical friction. Finally, the orbits of infalling satellites are more radial at high redshift, which further shortens the merger time-scale (Wetzel 2011). It should be noted that, while the remainder of this work posits that the satellite is accreted at redshift 8, this is by no means a unique solution.

To determine the properties of the Milky Way at this epoch, we assume that it grows according to the exponential halo model from McBride et al. (2009):

$$M(z) = M_{z=0}(1+z)^\beta \exp\left(-\ln 2 \frac{z}{z_f}\right), \quad (1)$$

where  $M_{z=0}$  is the current halo mass and  $z_f$  is the formation redshift, defined as the redshift at which the halo has grown to half its current mass. Adopting the properties for the Milky Way at  $z_f = 1$  as  $M_{z=0} = 2 \times 10^{12} M_\odot$  and  $\beta = 0.25$ , the Milky Way's mass at  $z = 8$  can be estimated to be  $M_{\text{MW}} = 7 \times 10^9 M_\odot$ . Studies of cosmological *N*-body simulations have found that at the redshift considered, the concentration of dark matter haloes is very weakly dependent on mass (Zhao et al. 2003; Gao et al. 2008; Klypin et al. 2011). Following the methods outlined by Prada et al. (2011), we find that at  $z = 8$  a halo of this mass will have a concentration of  $c(z = 8) \sim 6$ . The halo virial radius in a  $\Lambda$ CDM cosmology is defined as the radius where the mean enclosed density is 96 times the critical density of the universe,  $\rho_{\text{crit}}$ . With the definition of  $\rho_{\text{crit}}$ :

$$\rho_{\text{crit}} = \frac{3H_0^2}{8\pi G} \left[ \Omega_\Lambda + (1+z)^3 \Omega_m \right], \quad (2)$$

where  $\Omega_\Lambda = 0.73$  is the fraction of energy density in the universe in vacuum energy, while  $\Omega_m = 0.27$  is the fraction of energy density in the universe in matter, and  $z$  is the redshift. We find that

the progenitor MW halo has a virial radius of  $\sim 6$  kpc. This implies the progenitor Milky Way halo will have a density at 10 pc of  $30 M_\odot/\text{pc}^3 \sim 10^6 \rho_{\text{crit}}$ .

It is important to note that while Eqn. 1 assumes a single, smoothly growing Milky Way halo, at these high-redshifts, mergers with other massive haloes are very common, and the halo grows in a step-wise fashion. (Diemand et al. 2007). Indeed, the entire picture of a single, virialized progenitor Milky Way halo is not strictly correct, and the ‘Milky Way’ at this redshift is more likely a set of several haloes, many of which have not yet decoupled from the Hubble flow to allow turnaround and collapse into a single virialized structure. Consequently, our assumption of a virialized NFW halo at the accretion redshift ( $z = 8$ ) must be recognized as an approximation made due to the limits of a semi-analytic approach.

## 2.2 Finding the Culprit Satellite

Broadly, we identify possible culprit satellites by integrating the orbits of infalling haloes within an analytic, but evolving Milky Way potential. As both the satellite and Milky Way evolve, we search for the satellites that reach the Inner Lindblad Resonance (ILR) at 150 pc roughly 10 Myr ago after losing over 95% of its initial orbital angular momentum. Of the satellites that survive until they plunge through the ILR, we preferentially select those that retain enough mass to perturb the gas there. The culprit satellite is characterized by the mass, radius and concentration, as well as the energy, angular momentum, infall radius and merger redshift of the orbit. We elaborate on the procedure below.

We adopt a merger redshift of  $\sim 8$ . In order to deliver the IMBH to the GC a mere 2–7 Myr ago, the proposed merger redshift implies that the satellite orbit decayed over a time-scale of about 13 Gyr. At such a high redshift, the IMBH and satellite had very little time to evolve before being accreted by the Milky Way, making the pair a ‘fossil’ of the dark ages before reionization (Ricotti & Gnedin 2005; Gnedin & Kravtsov 2006).

We rely on cosmological *N*-body simulations to constrain the initial conditions of the orbit. These inform us that at the present epoch, satellites are preferentially accreted on very eccentric orbits, with a distribution peak at about  $e = 0.85$  (Benson 2005; Wang et al. 2005; Zentner et al. 2005; Khochfar & Burkert 2006; Ghigna et al. 1998; Tormen et al. 1997). At higher redshifts the satellite orbits are characterized by even higher eccentricities, albeit, in both cases the distribution peaks are broad. Seemingly independent of redshift, a typical satellite is accreted at the virial radius with a total velocity,  $|\vec{v}_{\text{sat}}| = 1.15v_{\text{vir}}$  ( $v_{\text{vir}}$  is the circular velocity at the virial radius of the primary galaxy) that marks it as barely bound (Benson 2005; Wetzel 2011). Motivated by these results, we select an orbit that has  $|\vec{v}_{\text{sat}}| = 1.15v_{\text{vir}}$  at the virial radius of the primary and an eccentricity of 0.9, consistent with expectations for the eccentricity distribution peak at  $z = 8$  (Wetzel 2011).

Starting with the above total velocity and eccentricity, we calculate the orbital decay for a range of satellite masses placed at the virial radius of the primary. For a given initial position at the virial radius, the azimuthal and radial components of the satellite's initial velocity within the orbital plane are calculated in terms of the eccentricity ( $e$ ) and total velocity ( $|\vec{v}_{\text{sat}}|$ ) as:

$$v_\phi = \frac{v_{\text{vir}}}{|\vec{v}_{\text{sat}}|} \sqrt{\frac{GM_{\text{MW}}}{r_{\text{vir}}}(1-e^2)} \quad \text{and} \quad v_r = \sqrt{|\vec{v}_{\text{sat}}|^2 - v_\phi^2}. \quad (3)$$

We adopt an analytic model of the Milky Way that includes a central SMBH, Miyamoto-Nagai thin disc (Miyamoto & Nagai 1975), a spherical Hernquist bulge (Hernquist 1990), and an NFW

halo (Navaro, Frenk, & White 1997). To mimic a young Milky Way, we use Eqn. 1 to set the halo mass. We set the virial radius using the mass and the critical density at the starting redshift in Eqn. 2, and we initialize the concentration using Prada et al. (2011). We assume that the mass and size of the baryonic components change in the same way as the halo does; this is not true in detail, but allows us to convert the known present-day Milky Way parameters to the starting redshift. Our current Milky Way mass model is similar to analytic models best-fit to rotation curve data (e.g. Widrow & Dubinski 2005; Dehnen & Binney 1998)  $z=0$  disc mass is  $5 \times 10^{10} M_{\odot}$ , the disc scale length is 3 kpc and, and the disc scale height is 300 pc. For the bulge, we set a current epoch bulge mass of  $8 \times 10^9 M_{\odot}$  and scale length of 0.7 kpc.

We integrate the orbits using a fourth-order Runge-Kutta method to step the satellite's position and velocity forward in time. At each timestep, we adjust the analytic Milky Way model using the method described above. We calculate the acceleration of the satellite due to this evolving analytic potential, and we include Chandrasekhar dynamical friction (Chandrasekhar 1943), as well as mass loss from the satellite due to tidal stripping and disc shocks. The acceleration due to dynamical friction is calculated in the uniform density limit as

$$\left(\frac{d\vec{v}_{\text{sat}}}{dt}\right)_{\text{fric}} = -\frac{4\pi \ln \Lambda G^2 M_{\text{sat}} \rho_{\text{MW}}}{|\vec{v}_{\text{sat}}|^3} \times \dots \times \left[\text{erf}(\chi) - \frac{2\chi}{\sqrt{\pi}} e^{-\chi^2}\right] \vec{v}_{\text{sat}}, \quad (4)$$

where  $M_{\text{sat}}$  is the mass of the satellite,  $\rho_{\text{MW}}$  is the density of the Milky Way at the satellite's position,  $\ln \Lambda = \ln [1 + (M_{\text{MW}}/M_{\text{sat}})^2]$  is the Coulomb logarithm,  $\chi = |\vec{v}_{\text{sat}}|/\sqrt{2}\sigma$ , and  $\sigma = \sqrt{GM_{\text{MW}}/2R_{\text{MW}}}$  is the average velocity dispersion of the Milky Way halo.

At each step in the orbit, we calculate the local density of the Milky Way and we tidally strip the satellite to the Roche radius, where the density of the satellite is equal to the Milky Way background. We also model mass loss from disc shocking by removing

$$\Delta M_{\text{shock}} = \frac{5}{3} \frac{4}{GM_{\text{sat}} v_{\text{sat},z}^2} \left(\frac{dv_{\text{sat},z}}{dt}\right)_{\text{disc}}^2 \quad (5)$$

from the satellite's mass each time it passes through the Milky Way disc (Gnedin & Ostriker 1997). We neglect the stellar component of the satellite, since the baryon content of such low mass satellites is relatively uncertain, but likely to be very small (Gnedin 2000; Simon & Geha 2007; Ricotti et al. 2008).

We find that the most likely culprit is a satellite with a mass of  $M_{\text{sat}} \approx 2 \times 10^8 M_{\odot}$ . Modeling the satellite dark matter profile as an NFW halo, its corresponding concentration parameter at this redshift is about 6 (Prada et al. 2011), making the satellite's central density within the inner 10 pc  $\sim 10 M_{\odot}/\text{pc}^3 \sim 4 \times 10^5 \rho_{\text{crit}}$  or  $\sim 2 \times 10^4$  times the Milky Way's density at the virial radius. Including an IMBH in our satellite model would deepen its central potential and could aid in delivering the satellite core to the centre of the MW intact, although we did not include this effect in our calculations.

By the time the satellite has reached the inner 100 pc, it will have lost most of its mass, with  $\sim 2 \times 10^5 M_{\odot}$  remaining. Without direct hydrodynamic simulations, it is difficult to say how much damage this IMBH-embedded satellite core could do to the gas-rich inner Milky Way. In general, we expect the satellite to perturb the gas in the galactic centre, torquing it and transporting angular momentum through narrow resonances (Goldreich & Tremaine 1979); the classical rate of gas inflow from this process is proportional to the strength of the perturbation squared. However, when the sys-

tem has a significant asymmetric perturbation, the orbits begin to cross one another and gas piles up in shocks (Papaloizou & Pringle 1977). In this case, the radial inflow rate of gas from a global perturbation is linearly proportional to the strength of perturbation (Hopkins & Quataert 2011), and numerical simulations find the shocks induced by even a few % perturbation can destabilize the gas and drive gas inflow (Barnes & Hernquist 1991, 1996; Mihos & Hernquist 1996; Hopkins & Quataert 2010). To estimate the perturbation a  $\sim 2 \times 10^5 M_{\odot}$  satellite core could exert on the gas accumulated in a ring at the Inner Lindblad Resonance (ILR) of the Milky Way, we refer to Vesperini & Weinberg (2000), which explores the perturbation strength induced by galaxy flyby encounters. Using linear perturbation theory, Vesperini & Weinberg (2000) find that a flyby with a mass ratio of 10 and a pericentre at the half-mass radius will induce a strong perturbation in the density of the primary galaxy of order unity. Since the mass ratio of the inner Milky Way ( $\sim 10^8 M_{\odot}$ ) to the satellite remnant is 1000 (Lindqvist et al. 1992), we expect a perturbation of the order  $|a| \sim 0.01$  in the surface density. The linear relationship between gas inflow and perturbation amplitude derived by Hopkins & Quataert (2011),

$$\frac{dM_{\text{gas}}}{dt} = |a| \Sigma_{\text{gas}} R^2 \Omega, \quad (6)$$

can then be used to gauge the expected amount of gas inflow. Setting the perturbation amplitude to  $|a| \sim 0.01$ , the radius to  $R = 150$  pc (ILR), the rotation frequency to  $\Omega(R) = v_{\text{circ}}(R)/R = 0.62 \text{ Myr}^{-1}$  (Stark et al. 2004), and the gas surface density to  $\Sigma_{\text{gas}} = 500 M_{\odot}/\text{pc}^2$  based on observations of other barred galaxies (Jogee et al. 2005) and of the molecular ring in the MW GC (Molinari et al. 2011), yields a gas inflow rate of  $\sim 7 \times 10^4 M_{\odot}/\text{Myr}$ . Assuming this inflow rate over  $\sim 10$  Myr, we find that this satellite should be able to drive a net inflow of  $\sim 10^6 M_{\odot}$  of gas from the ILR.

### 2.3 Late-Type Stellar Mass Deficit and IMBH Mass

If the core in the distribution of late-type stars at the GC (Buchholz et al. 2009; Do et al. 2009) was scoured out by an IMBH-SMBH binary (Preto et al. 2011; Gualandris & Merritt 2012), the amount of stellar mass missing from the GC can be used to constrain the mass ratio of the black hole binary (Milosavljević & Merritt 2001; Gualandris & Merritt 2008; Merritt 2006). To determine this mass deficit we compare the stellar distribution inferred from observations with that expected for a dynamically relaxed system without a core. In terms of the number density of the late-type stellar population, the core can be represented by a broken power law

$$n_f(r) = n_0 \left(\frac{r}{r_0}\right)^{-\gamma_i} \left[1 + \left(\frac{r}{r_0}\right)^{\alpha}\right]^{(\gamma_i - \gamma)/\alpha}, \quad (7)$$

with  $n_0 = 0.21 \text{ pc}^{-3}$ ,  $r_0 = 0.21 \text{ pc}$ ,  $\gamma = 1.8$ ,  $\gamma_i = -1.0$ , and  $\alpha = 4$  (Merritt 2010). We adopt this description in our analysis but note that in presence of strong mass segregation the slopes can be steeper (Alexander & Hopman 2009; Preto & Amaro-Seoane 2010; Amaro-Seoane & Preto 2011). The observed distribution of stars outside of the 0.21 pc core radius is consistent with the Bahcall-Wolf profile ( $\propto r^{-1.75}$ , Bahcall & Wolf 1976) of a relaxed system as it would have existed prior to scattering by the IMBH-SMBH binary. We model the initial stellar cusp by extending the

$r^{-1.8}$  profile to smaller radii:

$$n_i(r) = n_0 \left( \frac{r}{r_0} \right)^{-\gamma}. \quad (8)$$

Assuming that the mass density profiles *before* and *after* the creation of the core are proportional to equations (8) and (7) respectively, we calculate the mass deficit as the integrated difference between the initial and final (observed) profiles. We normalize the profile given by Eqn. 7 such that integrating it over the inner parsec yields  $1.0 \pm 0.5 \times 10^6 M_\odot$ , the mass determined by Schödel et al. (2009), and obtain  $M_{\text{def}} \approx 2 \times 10^5 M_\odot$ .

It should be understood that this mass deficit can only be treated as an estimate. Although this calculation assumes the best fit core radius ( $r_0$ ) and inner slope ( $\gamma_i$ ) from Merritt (2010), the fit was not excellent ( $\chi^2 > 17$ ) and the estimated mass deficit is highly dependent on these parameters. In addition, this calculation assumes that core size (and therefore the mass deficit) has not changed significantly over time. This is consistent with a core scoured recently enough ( $\sim 10$  Myr) that relaxation has not yet had enough time to fill in the core ( $\sim 10$  Gyr; Merritt 2010). However, it is also possible that the core is an evolved system; this implies a larger core, more massive IMBH, and more dramatic scouring event in the distant past. In this case, the creation of the core would have been unrelated to the creation of the young GC stars or Fermi bubbles.

N-body merger simulations studying the relationship between the ratio of total stellar mass ejected to binary mass,  $M_{\text{def}}/(M_1 + M_2)$ , and binary mass ratio,  $q = M_1/M_2$ , have not yet been carried out for the mass deficit calculated here. In order to relate the two we use a semi-analytic formalism describing the interaction of massive black hole binaries with their stellar environment (Sesana et al. 2008) to place the upper and lower limits on the mass of the IMBH based on  $M_{\text{def}}$  inferred from observations.

It has been shown by numerical simulations (Baumgardt et al. 2006; Matsubayashi et al. 2007) and semianalytic models (Sesana et al. 2008), that an IMBH inspiralling in a stellar cusp surrounding a central SMBH starts to efficiently eject stars at a separation  $a_0$ , where the stellar mass enclosed in the IMBH orbit is of the order of  $2M_2$ . The ejection of bound stars causes an IMBH orbital decay of a factor of  $\approx 10$ , excavating a core of radius  $r_0 \approx 2a_0$  in the central stellar cusp, resulting in a mass deficit about  $3M_2$  (see Sesana et al. 2008, for details). Such orbital decay is in general insufficient to bring the IMBH in the efficient gravitational wave (GW) emission regime, unless its eccentricity grows to  $> 0.9$  during the shrinking process. It is also the case in this picture that the mass of the inspiralling IMBH inferred for a given mass deficit strongly depends on the eccentricity evolution of its orbit. In what follows, we consider both the high and low orbital eccentricity scenario and use them to place a bound on the plausible range of IMBH masses.

If the eccentricity grows efficiently, the IMBH depletes the central cusp, forms a core of a size  $\approx 2a_0$ , and merges due to GW emission on a time scale of only 1–10 Myr (Sesana et al. 2008). For a stellar distribution described by an isothermal sphere outside of the radius of influence of the SMBH,  $a_0 = 2q^{4/5}$  pc. Adopting the core radius of  $r_0 = 2a_0 = 0.21$  pc, we find  $q = 0.02$ , and an upper limit on the mass of the IMBH,  $M_2 = 8 \times 10^4 M_\odot$ . In this case, the mass evacuated from the stellar cusp by the IMBH is of the order of  $3M_2$  (Sesana et al. 2008), i.e.,  $\approx 2.5 \times 10^5 M_\odot$ , consistent with the stellar mass deficit measurement in the GC.

Alternatively, if the IMBH eccentricity does not grow significantly during the bound cusp erosion, further scattering of stars replenishing the binary loss cone is needed in order to evolve from

separation of  $a_0$  to the GW regime. Therefore, a circular orbit regime can be used to establish a lower limit on the mass of the IMBH, for a given mass deficit indicated by observations. We assume that in this case both  $r_0$  and  $M_{\text{def}}$  created in the cusp erosion phase are small (we justify this assumption below). In this scenario, the final  $r_0$  and  $M_{\text{def}}$  are reached as a consequence of the diffusion of the stars from the edge of the small core into the loss cone of the binary. The ejections of each star carry away an energy of the order  $(3/2)G\mu/a$  (Quinlan 1996), where  $\mu = M_1 M_2/M$ . We compute  $M_{\text{def}}$  by imposing:

$$\frac{3}{2} \frac{G\mu}{a} dM_{\text{def}} = \frac{GM_1 M_2}{2} d \frac{1}{a} \quad (9)$$

to get

$$M_{\text{def}} = \frac{M_1 + M_2}{3} \ln \frac{a_i}{a_f}, \quad (10)$$

where  $a_i$  is the hardening radius of the binary (radius at which the scattering of unbound stars becomes effective) and  $a_f$  is the separation at which the GW emission becomes efficient. Using equations (19) and (20) in Sesana (2010) to express  $a_i$  and  $a_f$ , it follows that,

$$M_{\text{def}} = \frac{M_1 + M_2}{3} \ln \frac{500 q^{4/5}}{F(e)^{1/5}}, \quad (11)$$

where  $F(e) = (1 - e^2)^{-7/2} (1 + 73/24 e^2 + 37/96 e^4)$ . Assuming for the purpose of this estimate that the binary remains circular throughout its evolution and imposing  $M_{\text{def}} = 2 \times 10^5 M_\odot$ , we find  $q = 5 \times 10^{-4}$  and a lower limit on the mass of the IMBH is  $M_2 = 2 \times 10^3 M_\odot$ <sup>1</sup>. An IMBH of such mass, would excavate a core of  $\approx 0.01$  pc, causing a mass deficit of  $\sim 3M_2 = 6 \times 10^3 M_\odot$  in the bound scattering phase and thus, justifying our earlier assumption that the diffusion of stars into the loss cone is the primary process that shapes the properties of the core in this case. Note that in the circular orbit scenario the time scale for the inspiral of the IMBH towards the GW regime is determined by the unknown rate of diffusion of the stars into the loss cone of the binary. Hence, depending on the time scale of relaxation processes this process could in principle lead to the IMBH-SMBH binary ‘‘hangup’’, i.e., a long lived ( $> 1$  Gyr) binary configuration at separation  $< r_0$  – tantamount to the classical ‘‘final parsec’’ problem (Begelman & Rees 1980). It is however possible that the binary will not stall in our specific case. The galactic centre in this phase will be described by a strongly perturbed, non-axisymmetric potential which allows stars to scatter into the loss cone efficiently (Merritt & Poon 2004; Berczik et al. 2006; Perets & Alexander 2008; Khan et al. 2011). Moreover, the orbit will occur in a relatively gas-rich environment, which can further aid the decay of the binary (Escala et al. 2005; Dotti et al. 2007; Cuadra et al. 2009). Finally, any extra stars brought in by the satellite would help the binary decay (see Miller 2002). Even under the assumption of a circular orbit, an efficient coalescence can occur on a time-scale of 10 Myr.

This analysis suggests that the observed mass deficit and core size are consistent with the IMBH mass in the range  $2 \times 10^3 M_\odot < M_2 < 8 \times 10^4 M_\odot$ , whereas the efficient eccentricity growth found in N-body simulations and semi-analytic models favor  $M_2 \gtrsim 10^4 M_\odot$ . Within this range, the time scale for the IMBH to create a core and merge with the SMBH can be as short as few Myr. On the other hand, a possibility that an IMBH may be still be

<sup>1</sup> Both numerical simulations and semi-analytic models however suggest that the eccentricity in the cusp erosion phase grows to  $> 0.9$ , in which case  $F(e) > 1000$  and  $q > 5 \times 10^{-3}$ , i.e.,  $M_2 > 2 \times 10^4 M_\odot$ .

lurking in the GC is not completely ruled out. We discuss the consequences of the latter scenario in the context of the observational constraints on the presence of a second black hole in the Galactic centre in § 3.

It is useful to consider whether a satellite galaxy with an initial mass of  $M_{\text{sat}} \sim 2 \times 10^8 M_{\odot}$  can host a  $\gtrsim 10^4 M_{\odot}$  IMBH. While there are no observational constraints for galaxies or black holes of this mass range, there are three leading theories for IMBH formation at high redshift: ‘direct collapse’ of metal-free, low angular momentum gas into a  $10^3 - 10^6 M_{\odot}$  black hole (Loeb & Rasio 1994; Begelman et al. 2008), an unstable supermassive star that collapses into a  $10^2 - 10^5 M_{\odot}$  black hole (Colgate 1967; Quinlan & Shapiro 1987; Baumgarte & Shapiro 1999), or a Population III star, which would leave behind seed black holes of  $\sim 1 - 10^3 M_{\odot}$  between redshift 30–12 (Madau & Rees 2001; Bromm et al. 2002; Wise & Abel 2008; Clark et al. 2011). Even if the IMBH in our satellite started as a low mass Pop III seed in a somewhat turbulent environment with a mass of  $\sim 5 M_{\odot}$  (Clark et al. 2011), it is plausible that it would reach the IMBH mass proposed here through a combination of gas accretion and black hole mergers (Holley-Bockelmann et al. 2010). In such a satellite galaxy, it would require less than one percent of the gas to accrete onto a low mass seed to form the IMBH  $\gtrsim 10^4 M_{\odot}$ .

Note that the massive seeds produced in a direct collapse typically favor more massive haloes than the one we have proposed as our culprit. This is because metal-free gas collapses most efficiently in haloes with  $T_{\text{vir}} > 10^4$  K, corresponding to  $M_{\text{vir}} > 10^8 M_{\odot} [(1+z)/10]^{3/2}$  (Bromm & Loeb 2003). In the context of the merger hypothesis choosing a slightly more massive satellite would push the accretion redshift closer to the present day, and as long as the resulting satellite merger is still a minor one, this does not significantly affect the outcome of our scenario.

## 2.4 Inflow of Gas and Gamma-ray Bubbles

As noted in § 2.1 the inspiral of a satellite galaxy can cause the inflow of a significant amount of gas towards the centre of the Galaxy (Noguchi 1988; Barnes & Hernquist 1996; Mihos & Hernquist 1996; Cox et al. 2008). One fraction of this gas could have given rise to the star formation in the Central, Arches, and Quintuplet clusters, which marked the epoch between 2–7 Myr ago in the central 50 pc of the Milky Way. All three clusters contain some of the most massive stars in the Galaxy and have inferred masses of  $\sim 10^4 M_{\odot}$  (Figer 2008). Assuming a ‘‘standard’’ star formation efficiency of 10% (Rownd & Young 1999), it follows that the amount of gas necessary to produce the stellar population of the three clusters is a few  $\times 10^5 M_{\odot}$ . Note that a sequence of strongly compressional events during the satellite-Milky Way merger could have given rise to a higher efficiency of star formation (Di Matteo et al. 2007), in which case the estimated mass of the gas represents an upper limit.

In this merger scenario, the remainder of the perturbed gas that did not form stars would be channeled towards the central parsec (Loose et al. 1982), and the fraction that is accreted into the SMBH could drive the energetic outburst of several Myr ago. The far-IR and millimeter observations indicate that  $\sim 10^4 M_{\odot}$  of the molecular gas continues to reside in the circumnuclear disc within the central  $\sim 1.5$  pc of the Galaxy (see Genzel et al. 2010, for review and references therein). The maximum amount of the remnant molecular gas that has not been accreted onto the SMBH can also be estimated based on its expected gravitational effect on the orbits of the stars residing within the inner 0.5 pc. In this case, the re-

quirement for stability of the stellar disc over its lifetime of 6 Myr poses a constraint on the mass of the molecular torus of  $< 10^6 M_{\odot}$  (Šubr et al. 2009).

On the other hand, the recent discovery of the two large gamma-ray bubbles extending from the GC above and below the galactic plane are compelling evidence of a relatively recent period of intense activity in the now quiet GC. The gamma-ray bubbles exhibit several striking properties: they are perpendicular and symmetric with respect to the plane of the Galaxy, have nearly uniform gamma-ray brightness across the bubbles, and well defined sharp edges (Dobler et al. 2010; Su et al. 2010). The gamma-ray emission from the bubbles is characterized by the hard energy spectrum and is most likely to originate from the inverse Compton scattering of the interstellar radiation field on the cosmic ray electrons – the same population of electrons deemed responsible for the diffuse synchrotron microwave radiation detected by the WMAP (Finkbeiner 2004; Dobler & Finkbeiner 2008). The sharp edges of the Fermi bubbles are also traced by the X-ray arcs discovered in the ROSAT maps (Snowden et al. 1997), suggested to be the remnants of shock fronts created by the expanding bubbles (Su et al. 2010; Guo & Mathews 2011).

The morphology, energetics, and emission properties of the Fermi bubbles favor the explanation that bubbles were created in a strong episode of energy injection in the GC in the last  $\sim 10$  Myr that followed an accretion event onto the SMBH (Su et al. 2010). Simulations by Guo & Mathews (2011) indicate that the bubbles could have been formed by a pair of bipolar jets that released a total energy of  $1 - 8 \times 10^{57}$  erg over the course of  $\sim 0.1 - 0.5$  Myr between 1 and 2 Myr ago. This explanation for the Fermi bubbles implies that  $\sim 10^4 M_{\odot}$  of material must have been accreted onto the SMBH at nearly the Eddington rate, assuming the accretion efficiency of 10% (Shakura & Sunyaev 1973; Davis & Laor 2011). Based on the range of models explored by Guo & Mathews (2011) it is possible to estimate that the amount of mass processed in such jets (i.e., the mass of the gas that fills the jet cavities) is as small as  $30 M_{\odot}$  and as large as  $3 \times 10^5 M_{\odot}$ .

This estimate, together with the gas that formed stars, the gas accreted onto the SMBH and the gas processed by the jets allows us to put a constraint on the total gas inflow into the central  $\sim 50$  pc of the Galaxy of  $\lesssim 10^6 M_{\odot}$ , consistent with the amount expected from the perturbation analysis of the stability of the ILR gas in the Milky Way.

## 3 DISCUSSION

### 3.1 How rare are satellite merger events?

We propose that the timeline began about 13 Gyr ago, when the proto Milky Way accreted a small satellite dark matter halo at the time when their haloes were physically closer and less massive. The satellite orbit decayed slowly and only reached the GC a few million years ago, after having been stripped of most its mass. The thinness of the Milky Way disc has often been used as an argument against a recent minor merger (Quinn, Hernquist, & Fullagar 1993; Sellwood, Nelson, & Tremaine 1998; Velázquez & White 1999); however, the proposed satellite is so minor, particularly by the time the orbit decays to 10 kpc, that the thin disc could have survived unscathed (Toth & Ostriker 1992; Walker et al. 1996; Taylor & Babul 2001; Hopkins et al. 2008, 2009).

Using the Extended Press-Schechter formalism (EPS) (Bond et al. 1991; Bower 1991; Lacey & Cole 1993;

Parkinson et al. 2008), we can estimate the number of satellite accretion events a typical Milky Way mass galaxy will undergo. We determined this on the basis of 100 realizations of an EPS merger tree that resulted in a base halo of  $2 \times 10^{12} M_{\odot}$  at  $z=0$ . In this calculation, we assumed WMAP5 parameters and summed over the haloes in the  $M_{\text{sat}} = 10^7 - 10^9 M_{\odot}$  mass range that merged with the main halo from  $z=7$  to  $z=0$ . We found a mean of 1745 such satellite accretion events, with a standard deviation of 425. However, about half of these accretions occur after  $z = 1$  — and are unlikely to have made it to the GC by  $z = 0$ . We confirmed that this number of satellite accretion events is consistent with expectations from the cosmological simulations by comparing to one of our N-body simulations of a  $50 \text{ Mpc}^3$  volume described in Sinha & Holley-Bockelmann (2012).

Figure 1 illustrates one realization of the current distribution of accreted satellites in the mass range  $M_{\text{sat}} = 10^7 - 10^9 M_{\odot}$ . We used the EPS technique described above to define the number of accreted satellites in this mass range at each integer step in redshift from  $z=7$  to  $z=0$ . To define the orbit of each satellite as it is accreted, we randomly selected from the energy and angular momentum distributions at each redshift using the expressions 7–9 in (Wetzel 2011). As in section 2, we integrated orbits of the satellites from the accretion epoch to the present day, scaling the Milky Way mass and size to the redshift of accretion using Eqn. 1. Figure 1 shows the inner 40 kpc of the current-day Milky Way; approximately 85% of the accreted satellites are at separations larger than 40 kpc, and only 5 reached the GC and merged with the SMBH. We estimate the surface brightness of the satellites assuming that the baryons are confined to a radius within the dark matter halo ten times smaller than the satellite virial radius. We infer the initial star fraction from Ricotti & Gnedin (2005) and assume a total mass-to-light ratio of  $\sim 300$  (Strigari et al. 2008) for the bound stars that remain after tidal stripping.

While it is very clear that not all of the small satellites can reach the GC, what fraction does is a question of some subtlety. Galaxy merger time-scales cited in the literature, particularly for the small mass ratios considered here, span a wide range. The key to the uncertainties is the treatment of dynamical friction: most semi-analytic works, including this one, rely on the dynamical friction formalism as described by Chandrasekhar (1943) but change the Coulomb logarithm to account for inhomogeneous or anisotropic systems (Peñarrubia et al. 2004; Just & Peñarrubia 2005), or to include mass loss (Taylor & Babul 2001; Velázquez & White 1999). This approach has been shown to underestimate the decay time in pure dark matter simulations (Colpi et al. 1999; Boylan-Kolchin et al. 2008). On the other hand, the presence of gas can dramatically decrease the orbital decay time of a satellite by efficiently dissipating its orbital energy throughout the system (Ostriker 1999; Sánchez-Salcedo & Brandenburg 1999) — thus, making the Chandrasekhar formula a significant overestimate. Compounding the issue, linear perturbation theory and limited N-body experiments indicate that resonant heating caused by orbits in the satellite galaxy that are commensurate with the orbit of the satellite about the GC can enhance mass loss and can change the angular momentum of the orbit in non-trivial ways (Weinberg 1997; Choi et al. 2009). Although the Milky Way has likely accreted over a thousand of these small satellites, it is uncertain how often they reached the galactic centre. It is however plausible that the GC has experienced a handful of these accretion events spread over its lifespan. Despite the uncertainty that arises in the mass of our culprit satellite due to the imprecise dynamical friction time-scale, the scenario itself remains viable, because other constraints

on satellite mass (satellite evaporation, disc disruption) are flexible so long as the merger time-scale remains less than the age of the universe.

### 3.2 Hypervelocity stars and stellar core

While the properties of the newly formed stars and perturbed gas were dictated by the accreted satellite, the IMBH was responsible for carving out the old stellar population. As a gravitationally bound binary IMBH-SMBH formed and decayed, it scoured out  $2 \times 10^5 M_{\odot}$  of the relaxed old and initially cuspy stellar population. Many of these stars could have been ejected from the GC as hypervelocity stars (HVSs; Brown et al. 2005; Baumgardt et al. 2006), though most may simply have received enough energy to traverse the inner parsec. Simulations of IMBH-SMBH binaries in stellar environments indicate that HVSs are created in a short burst which lasts only a few Myr in case of a  $\sim 10^4 M_{\odot}$  IMBH (Baumgardt et al. 2006; Sesana et al. 2008). In the context of our picture we predict that this event created  $\sim 10^3$  hypervelocity stars that, if they were ejected at about  $1000 \text{ km s}^{-1}$  (Baumgardt et al. 2006), ought to lie  $\sim 10 \text{ kpc}$  from the GC today. It is worth noting that about a dozen of HVSs observed in the Galactic halo thus far have travel times that span 60–240 Myr and appear to be consistent with a continuous ejection model (Brown 2008; Brown et al. 2009; Tillich et al. 2009; Irrgang et al. 2010) and not with the IMBH-SMBH binary picture (Brown 2008; Sesana et al. 2008). Along similar lines, the spatial and velocity distribution of the current observed HVSs seem to be inconsistent with a IMBH-SMBH slingshot origin (Sesana et al. 2007).

The large size of the observed GC core,  $r_0 = 0.21 \text{ pc}$ , could be seen as a challenge to any scenario involving 3-body scattering, since state of the art high resolution direct N-body simulations that modeled the ejection of hypervelocity stars from a SMBH-IMBH binary in the galactic centre never generated a core larger than 0.02 parsecs (Baumgardt et al. 2006). However, there are several effects that could conspire to cause the simulated core size to be a lower limit. First, the mass of the simulated SMBH in Baumgardt et al. (2006) is  $3 \times 10^6 M_{\odot}$ , which would eject fewer stars than somewhat more massive Milky Way SMBH. Second, the density profile was sharply curtailed by a factor of  $(1+r^5)$  in order to minimize the number of stars far from the SMBH; this makes the spatial distribution of stars in the simulated nuclear star cluster more centrally peaked relative to that in the GC, which can also result in a smaller core. In general, though, it is important to note that the size of the scoured core is a property that sensitively depends on the density, the eccentricity, and kinematic structure of the GC or on assumptions in the model used to represent it.

### 3.3 Has IMBH-SMBH binary merged?

We now return to the question whether the IMBH-SMBH binary has already merged or whether the IMBH could still be lurking in the GC. As discussed in § 2.3, the N-body and semi-analytic modeling of the GC favor the evolutionary scenarios in which the inspiral and coalescence of the SMBH with a  $M_2 \gtrsim 10^4 M_{\odot}$  IMBH is relatively efficient. Moreover, there is currently no empirical evidence for a second black hole in the central parsec. In order to be consistent with the observations, the IMBH present in the GC would have to have a mass  $\sim 10^3 - 10^{4.5} M_{\odot}$  and be either very close ( $\leq 10^{-3} \text{ pc}$ ) or at  $> 0.1 \text{ pc}$  from the SMBH (Reid & Brunthaler 2004; Gualandris & Merritt 2009; Gualandris, Gillessen & Merritt

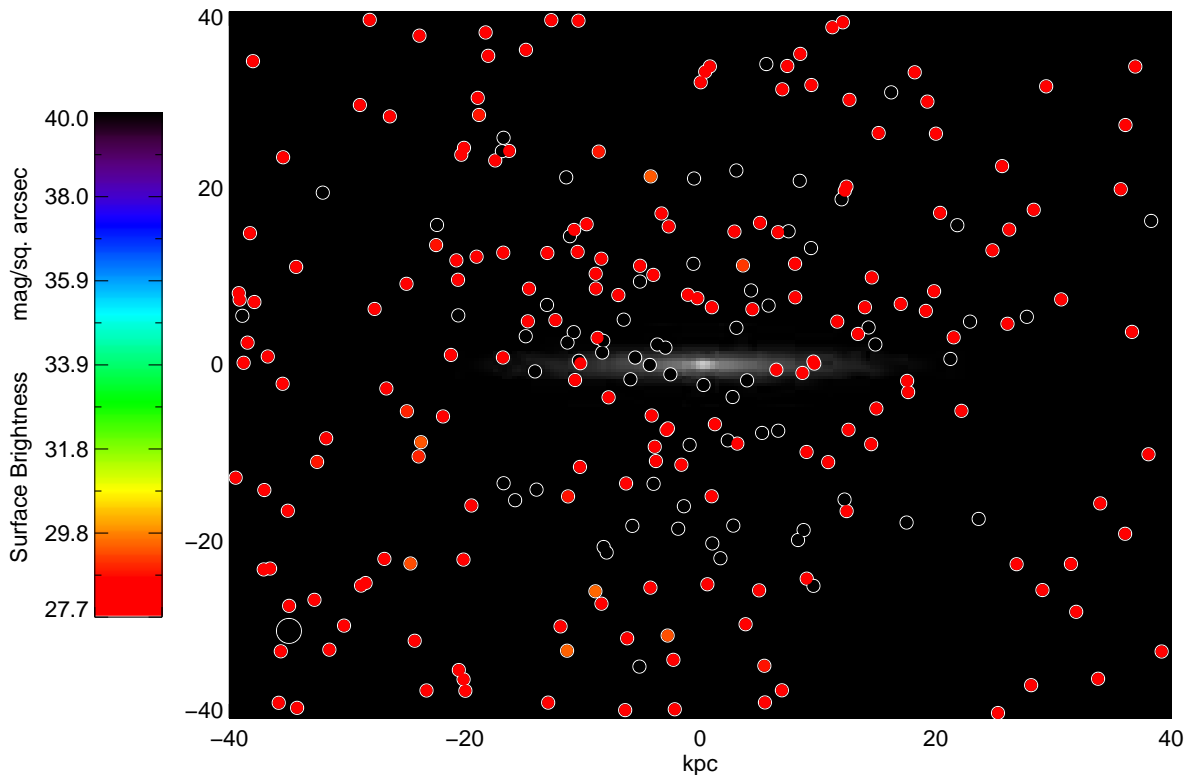


**Figure 1.** Distribution of accreted low mass satellites at the present day. The inner 40 kpc region of the Milky Way disc is shown in greyscale with current accreted satellite positions overlotted. The color maps to the surface brightness, and the relative size corresponds to the tidal radius of the satellite. Note that the circle size is not to scale and that none of these satellites would be observable above the background. Also note that satellites that have merged with SMBH or completely disrupted are not plotted.

2010; Genzel et al. 2010). An IMBH in this mass range that reaches a separation of  $10^{-4}$  pc would merge with the SMBH in less than 10 Myr due to the emission of GWs, thus severely restricting the amount of parameter space where the IMBH and SMBH can exist in a long lived binary configuration. Nevertheless, given the uncertainties in the binary mass ratio, eccentricity, and the structure of the initial stellar cusp, the presence of an IMBH in the GC cannot be entirely ruled out at this point.

If on the other hand, the IMBH and SMBH coalesced several million years ago, one possible signature of this event could be a SMBH recoil caused by the asymmetric emission of GWs (Peres 1962; Bekenstein 1973). Current astrometric observations of the reflex motion of the SMBH put strong constraints on the allowed recoil velocity; the SMBH cannot have velocity with respect to the Central cluster larger than 3.5 km/s (within  $1\sigma$  error), at the distance of the GC (Yelda et al. 2010). Similarly, Reid & Brunthaler (2004) constrain the peculiar motion of Sgr A\* in the plane of the Galaxy to  $-18 \pm 7$  km/s and perpendicular to the Galactic plane to  $-0.4 \pm 0.9$  km/s, where quoted uncertainties are  $1\sigma$  errors. There is however a caveat with respect to the interpretation of the SMBH reflex motion: if the reference frame in which the reflex motion is measured is based on the nearby gas and stars bound to the SMBH, the resulting relative velocity of the SMBH will be zero because in this case, the stars and the gas move together with the SMBH as long as their orbital velocity is higher than the that of the reflex

motion. The radio and near-infrared reference frames in Yelda et al. (2010) are defined based on the nearby stars orbiting around the SMBH and are thus a subject to this caveat. The measurement of Reid & Brunthaler (2004) is however carried out in the reference frame defined by the extragalactic radio sources and can be used to test the recoil hypothesis.

For  $10^4 M_\odot$  IMBH the black hole merger can give rise to a modest recoil velocity of about 80 m/s, assuming that the IMBH is not spinning rapidly. The recoil velocity magnitude in this case scales as  $\propto q^2$  (Campanelli et al. 2007; Baker et al. 2008), thus implying that the coalescence of the SMBH with a slowly spinning IMBH more massive than  $1.5 \times 10^5 M_\odot$  can be ruled out based on larger of the observational constraints, as long as damping of the recoil motion of a remnant SMBH is inefficient on the time scale of several million years. More stringent constraints on the mass of the IMBH, based on the motion of the SMBH perpendicular to the Galactic plane, can be placed given the (unknown) orientation of the orbital plane of the binary before the merger in addition to the binary mass ratio and the spin vector of the IMBH.

### 3.4 Orientation of the SMBH spin axis

The nearly perpendicular orientation of the spin axis of the SMBH to the Galactic disc plane, indicated by the orientation of the observed gamma-ray bubbles and jets in simulations of



Guo & Mathews (2011), implies that the evolution of the SMBH spin has been determined by accretion from the Galactic gas disc rather than random accretion events with isotropic spatial distribution. Such events would include tidal disruptions of stars and giant molecular clouds triggered by the satellite inspiral and a merger with the satellite IMBH which orbital plane in principle may not be aligned with the plane of the Galaxy. It is thus interesting to consider whether a sequence of such accretion events can exhibit a cumulative torque on the SMBH sufficient to re-orient its spin axis, assuming that before the merger with a satellite galaxy it was perpendicular to the Galactic plane.

Consider first the effect of episodic gas accretion resulting from multiple tidal disruption events. Chen et al. (2009, 2011) show that three-body interactions between bound stars in a stellar cusp and a massive binary with properties similar to the IMBH-SMBH considered here can produce a burst of tidal disruptions, which for a short period of time ( $\sim 0.1$  Myr) can exceed the tidal disruption rate for a single massive black hole by two orders of magnitude, reaching  $\dot{N} \sim 10^{-2} \text{ yr}^{-1}$ . This implies that in the process of the IMBH inspiral the SMBH could have disrupted  $\sim 10^3$  stars. A key element in this consideration follows from the finding by Natarajan & Pringle (1998) and Natarajan & Armitage (1999) that the orientation of the spin axis of a SMBH is very sensitive to the angular momentum of the accreted gas: namely, accretion of a mere few % in mass of a SMBH can exert torques that change the direction but not the magnitude of the spin of a black hole. Because each in a sequence of random accretion events imposes an infinitesimal change in the orientation of the SMBH spin axis, collectively they can cause the spin axis to perform a random walk about its initial orientation. Thus, the magnitude of the effect scales with the number of disrupted stars and their mass as  $\sim \sqrt{N} m_*$ . Since this is much less than few percent of  $M_1$ , the cumulative effect of tidal disruption events on the orientation of the spin axis of the SMBH will be negligible.

This conclusion is reinforced by an additional property of post-tidal disruption accretion discs: they are compact in size and usually confined to the region of a size  $\text{few} \times r_t$ , where  $r_t \approx r_* (M_1/m_*)^{1/3}$  is the tidal disruption radius of a star and  $r_*$  is the stellar radius (Rees 1988). Such small accretion discs effectively act as very short lever arms for torques acting on the spin axis of the SMBH, thus further reducing the efficiency of this process (Natarajan & Pringle 1998).

Similar conclusions can be reached about the tidally disrupted molecular clouds and gas flows that plunge towards the SMBH on nearly radial orbits as a consequence of perturbations excited by the satellite galaxy. In section § 2.4 we estimated that the amount of mass accreted by the SMBH is  $\sim 10^4 M_\odot$ . A modest mass, combined with the small circularization radius of the gas accretion disc is insufficient to cause a significant change in the SMBH spin orientation. Even “accretion” of a spinning IMBH is not expected to noticeably influence the spin orientation of the remnant SMBH. The large mass ratio of the binary ensures that the final contribution of the IMBH’s spin and orbital angular momentum to the final spin of the SMBH is small, as long as the pre-merger SMBH has a moderate initial spin,  $> \text{few} \times 0.1$ , in terms of the dimensionless spin parameter (Barausse & Rezzolla 2009). Hence, coalescence with the IMBH would not have had a significant effect on the SMBH spin axis orientation.

In summary, the torques from the accretion of tidally disrupted stars, gas, and the IMBH in the aftermath of the satellite inspiral will be insufficient to change the orientation of the SMBH spin axis as long as the SMBH spin is  $> \text{few} \times 0.1$ . It follows that the

perpendicular orientation of the spin axis has been set by the physical processes before the merger with the satellite, and most likely by the accretion of gas from the Galactic disc.

## 4 CONCLUSIONS

A range of theoretical arguments and observational evidence could indicate a satellite infall event within our GC which triggered a brief epoch of strong star formation and AGN activity millions of years ago. When coupling the newest data – on the Fermi bubble and the dearth of late-type stars – to the well-established features of the GC such as the cuspy early-type stellar population, a timeline of the recent dynamical events in the galactic centre emerges.

While the case for a merger of the Milky Way with a satellite galaxy is not beyond reproach, it is a plausible explanation that naturally accounts for both the late- and early-type stellar distributions and the recent violent past of Sgr A\*. This event may not be unique in the evolution of the Milky Way; indeed N-body simulations of the growth of Milky Way-mass galaxies suggest that the present epoch is rife with mergers of relic satellite galaxies with the galactic centre, occurring at a rate of one per few Gyr (Diemand et al. 2007; Sinha & Holley-Bockelmann 2012). This implies that there may have been other bursts of hypervelocity star ejections, which can seed a population of “intragroup stars” farther out in the halo of the Galaxy. Interestingly, we see tentative evidence in the SDSS archive for a potential set of very late M giants at  $\sim 300$  kpc, outside the virial radius of our galaxy (Palladino et al. 2012). Although a followup observation is needed to ensure that these intragroup candidates are not L dwarfs, if these do prove to be very distant giants, they may provide supporting evidence of a previous minor-merger induced burst of ejected stars  $\sim 10^8$  years ago.

Along similar lines, if satellite infall induced activity is common, then there may be a subset of spiral galaxies which exhibits the signs of the recent onset of the accretion-powered jets. While the longer term X- and  $\gamma$ -ray signatures of jets expanding into the intragalactic medium may be too faint to observe in galaxies other than the Milky Way, relatively bright and short lived radio-jets ( $\sim 0.1$  Myr; Guo & Mathews 2011) may be present in a fraction of up to  $\sim 10^{-4}$  Milky-Way-like spirals, assuming the minor merger rate cited above. Some of these galaxies may be observed serendipitously, during the transient phase associated with the onset of a powerful jet, similar to the case of the previously inactive galaxy J164449.3+573451 that was recently detected by the Swift observatory as a powerful source of beamed emission (Burrows et al. 2011). If it can be shown that such a sequence of events occurred in the not so distant past in our Galaxy, it would forever change the paradigm of the Milky Way as an inactive galaxy with an underluminous central SMBH.

## ACKNOWLEDGMENTS

We thank our referee for thoughtful suggestions that significantly improved this work. We thank Cole Miller, Melvyn Davies, Jorge Cuadra and Rainer Schödel for insightful discussions. K.H-B., T.B., P.A-S. and A.S. also acknowledge the hospitality of the Aspen Center for Physics, where the work was conceived and carried out. K.H-B. acknowledges the support of a National Science Foundation Career Grant AST-0847696, and a National Aeronautics and Space Administration Theory grant NNX08AG74G as well as the supercomputing support of Vanderbilt’s Advanced Center for

Computation Research and Education, and NASA's Pleiades and Columbia clusters. Support for T.B. was provided by the National Aeronautics and Space Administration through Einstein Postdoctoral Fellowship Award Number PF9-00061 issued by the Chandra X-ray Observatory Center, which is operated by the Smithsonian Astrophysical Observatory for and on behalf of the National Aeronautics Space Administration under contract NAS8-03060. Support for M.L. was provided by a National Science Foundation Graduate Research Fellowship.

## REFERENCES

- Alexander T., Hopman C., 2009, *ApJ*, 697, 1861
- Amaro-Seoane P., Preto M., 2011, *Classical and Quantum Gravity*, 28, 094017
- Bahcall, J. N. & Wolf, R. A. 1976, *ApJ*, 209, 214
- Baker, J. G., Boggs, W. D., Centrella, J., Kelly, B. J., McWilliams, S. T., Miller, M. C., & van Meter, J. R. 2008, *ApJ*, 682, L29
- Barausse, E., & Rezzolla, L. 2009, *ApJ*, 704, L40
- Barnes, J. E. & Hernquist, L. 1991, *ApJ*, 370, L65
- Barnes, J. E., & Hernquist, L. 1992, *ARA&A*, 30, 705
- Barnes, J. E., & Hernquist, L. 1996, *ApJ*, 471, 115
- Bartko, H., et al. 2010, *ApJ*, 708, 834
- Baumgarte, T. W., & Shapiro, S. L. 1999, *ApJ*, 526, 941
- Baumgardt, H., Gualandris, A., & Portegies Zwart, S. 2006, *MNRAS*, 372, 174
- Begelman, M. C., Blandford, R. D., & Rees, M. J. 1980, *Nature*, 287
- Begelman, M. C., Rossi, E. M., & Armitage, P. J. 2008, *MNRAS*, 387, 1649
- Bekenstein, J. D. 1973, *ApJ*, 183, 657
- Benson, A. J. 2005, *MNRAS*, 358, 551
- Berczik, P., Merritt, D., Spurzem, R., & Bischof H. P. 2006, *ApJ*, 624, 21
- Bond, J. R., Cole, S., Efstathiou, G., & Kaiser, N. 1991, *ApJ*, 379, 440
- Bonnell, I., & Rice, W. 2008, *Science*, 321, 1060
- Bower, R. G. 1991, *MNRAS*, 248, 332
- Boylan-Kolchin, M., Ma, C.-P., & Quataert, E. 2004, *ApJ*, 613, L37
- Boylan-Kolchin, M., Ma, C.-P., & Quataert, E. 2008, *MNRAS*, 383, 93
- Bromm, V., & Loeb, A. 2003, *ApJ*, 596, 34
- Bromm, V., Coppi, P. S., & Larson, R. B. 2002, *ApJ*, 564, 23
- Brown, W. R., Geller, M. J., Kenyon, S. J., & Kurtz, M. J. 2005, *ApJ*, 622, L33
- Brown, W. R. 2008, *arXiv:0811.0571*
- Brown, W. R., Geller, M. J., & Kenyon, S. J. 2009, *ApJ*, 690, 1639
- Buchholz, R. M., Schödel, R., & Eckart, A. 2009, *A&A*, 499, 483
- Bullock, J. S., et al. 2001, *MNRAS*, 321, 559
- Burrows, D. N., et al. 2011 (*arXiv:1104.4787*)
- Callegari, S., Kazantzidis, S., Mayer, L., Colpi, M., Bellovary, J. M., Quinn, T., & Wadsley, J. 2011, *ApJ*, 729, 85
- Campanelli, M., Lousto, C., Zlochower, Y., & Merritt, D. 2007, *ApJ*, 659, L5
- Chandrasekhar, S. 1943, *ApJ*, 97, 255
- Chen, X., Madau, P., Sesana, A., & Liu, F. K. 2009, *ApJ*, 697, L149
- Chen, X., Sesana, A., Madau, P., & Liu, F. K. 2011, *ApJ*, 729, 13
- Cheng, K. S., Chernyshov, D. O., Dogiel, V. A., Ko, C. -, & Ip, W. -. 2011, *ApJ*, 731, L17
- Choi, J.-H., Weinberg, M. D., & Katz, N. 2009, *MNRAS*, 400, 1247
- Clark, P. C., Glover, S. C. O., Klessen, R. S., & Bromm, V. 2011, *ApJ*, 727, 110
- Colgate, S. A. 1967, *ApJ*, 150, 163
- Colpi, M., Mayer, L., & Governato, F. 1999, *ApJ*, 525, 720
- Cox, T. J., Jonsson, P., Somerville, R. S., Primack, J. R., & Dekel, A. 2008, *MNRAS*, 384, 386
- Crocker, R. M., Jones, D. I., Aharonian, F., Law, C. J., Melia, F., Oka, T., & Ott, J. 2011, *MNRAS*, 413, 763
- Cuadra, J., Armitage, P. J., Alexander, R. D., & Begelman, M. C. 2009, *MNRAS*, 393, 1423
- Davis, S. W. & Laor, A. 2011, *ApJ*, 728, 98
- Dehnen, W., & Binney, J. 1998, *MNRAS*, 294, 429
- Diemand, J., Kuhlen, M., & Madau, P. 2007, *ApJ*, 667, 859
- Di Matteo, P., Combes, F., Melchior, A.-L., & Semelin, B. 2007, *A&A*, 468, 61
- Do, T., Ghez, A. M., Morris, M. R., Lu, J. R., Matthews, K., Yelda, S., & Larkin, J. 2009, *ApJ*, 703, 1323
- Dobler, G., Finkbeiner, D. P., Cholis, I., Slatyer, T., & Weiner, N. 2010, *ApJ*, 717, 825
- Dobler, G., & Finkbeiner, D. P. 2008, *ApJ*, 680, 1222
- Dotti, M., Colpi, M., Haardt, F., & Mayer, L. 2007, *MNRAS*, 379, 956
- Escala, A., Larson, R. B., Coppi, P. S., & Mardones, D. 2005, *ApJ*, 630, 152
- Faber, S. M., et al. 1997, *AJ*, 114, 1771
- Ferrarese et al. 2006, *ApJS*, 164, 334
- Figer, D. F., et al. 2000, *ApJ*, 533, L49
- Figer, D. F. 2008 (*arXiv:0803.1619*)
- Finkbeiner, D. P. 2004, *ApJ*, 614, 186
- Gao, L. et al. 2008, *MNRAS*, 387, 536
- Genzel, R., et al. 2003, *ApJ*, 594, 812
- Genzel, R., Eisenhauer, F., & Gillessen, S. 2010, *Reviews of Modern Physics*, 82, 3121
- Ghigna, S., et al. 1998, *MNRAS*, 300, 146
- Gilmore, G., Wyse, R. F. G., & Norris, J. E. 2002, *ApJ*, 574, L39
- Gnedin, N. Y. 2000, *ApJ*, 542, 535
- Gendin, N. Y. & Kravtsov, A. V. 2006, *ApJ*, 645, 1054
- Gnedin, O. Y. & Ostriker, J. P. 1997, *ApJ*, 474, 223
- Goldreich, P., & Tremaine, S. 1979, *ApJ*, 233, 857
- Graham, A. W. 2004, *ApJ*, 613, L33
- Gualandris, A., & Merritt, D. 2008, *ApJ*, 678, 780
- Gualandris, A., & Merritt, D. 2009, *ApJ*, 705, 361
- Gualandris, A., Gillessen, S., & Merritt, D. 2010, *MNRAS*, 409, 1146
- Gualandris, A., & Merritt, D. 2012, *ApJ*, 744, 74
- Guo, F. & Mathews, W. G. 2011, *Draft*
- Hansen, B. M. S., & Milosavljević, M. 2003, *ApJ*, 593, L77
- Hernquist, L. 1990, *ApJ*, 356, 359
- Holley-Bockelmann, K., Micic, M., Sigurdsson, S., & Rubbo, L. J. 2010, *ApJ*, 713, 1016
- Hopkins, P. F. et al. 2008, *ApJ*, 688, 757
- Hopkins, P. F., Cox, T. J., Younger, J. D., & Hernquist, L. 2009, *ApJ*, 691, 1168
- Hopkins & Hernquist 2010, *MNRAS*, 407, 447
- Hopkins, P. F. & Quataert, E. 2010, *MNRAS*, 407, 1529
- Hopkins, P. F. & Quataert, E. 2011, *MNRAS*, 415, 1027
- Inui, T., Koyama, K., Matsumoto, H., & Tsuru, T. G. 2009, *PASJ*, 61, S241
- Irrgang, A., Przybilla, N., Heber, U., Nieva, M. F., & Schuh, S. 2010, *ApJ*, 711, 138

- Jogee, S., Scoville, N., & Kenny, J. D. P. 2005, *ApJ*, 630, 837  
 Just, A., & Peñarrubia, J. 2005, *A&A*, 431, 861  
 Khan, F. M., Just, A., & Merritt, D. 2011, *ApJ*, 732, 89  
 Khochfar, S., & Burkert, A. 2006, *A&A*, 445, 403  
 Klypin, A. A., Trujillo-Gomez, S., & Primack, J. 2011, *ApJ*, 740, 102  
 Kormendy, J., & Bender, R. 2009, *ApJ*, 691, L142  
 Krabbe, A., et al. 1995, *ApJ*, 447, L95  
 Lacey, C., & Cole, S. 1993, *MNRAS*, 262, 627  
 Lindqvist, M., Habing, H. J., & Winnberg, A. 1992, *A&A*, 259, 118  
 Loeb, A., & Rasio, F. A. 1994, *ApJ*, 432, 52  
 Loose, H. H., Kruegel, E., & Tutukov, A. 1982, *A&A*, 105, 342  
 Madau, P., & Rees, M. J. 2001, *ApJ*, 551, L27  
 Mapelli, M., Hayfield, T., Mayer, L., & Wadsley, J. 2012, *ApJ*, 749, 168  
 Matsubayashi, T., Makino, J., & Ebisuzaki, T. 2007, *ApJ*, 656, 879  
 McBride, J., Fakhouri, O., & Ma, C. 2009, *MNRAS*, 398, 1858  
 Merritt, D. 2006, *ApJ*, 648, 976  
 Merritt, D. 2010, *ApJ*, 718, 739  
 Merritt, D. & Cruz, F. 2001, *ApJ*, 551, L41  
 Merritt, D. & Poon, M. Y. 2004, *ApJ*, 606, 788  
 Merritt, D., Gualandris, A., & Mikkola, S. 2009, *ApJ*, 693, L35  
 Micic, M., Holley-Bockelmann, K., & Sigurdsson, S. 2011, *MNRAS*, 414, 1127  
 Mihos, J. C. & Hernquist, L. 1996, *ApJ*, 464, 641  
 Miller, M. C. 2002, *ApJ*, 581, 438  
 Milosavljević, M., & Merritt, D. 2001, *ApJ*, 563, 34  
 Miyamoto, M. & Nagai, R. 1975, *PASJ*, 27, 533  
 Molinari, S., Bally, J., Noriega-Crespo, A., et al. 2011, *ApJ*, 735, L33  
 Noguchi, M. 1988, *A&A*, 203, 259  
 Natarajan, P., & Armitage, P. J. 1999, *MNRAS*, 309, 961  
 Natarajan, P., & Pringle, J. E. 1998, *ApJ*, 506, L97  
 Navarro, J. F., Frenk, C. S., & White, S. D. M. 1997, *ApJ*, 490, 493  
 Ostriker, E. C. 1999, *ApJ*, 513, 252  
 Palladino, L. E., Holley-Bockelmann, K., Morrison, H., et al. 2012, *AJ*, 143, 128  
 Papaloizou, J., & Pringle, J. E. 1977, *MNRAS*, 181, 441  
 Parkinson, H., Cole, S., & Helly, J. 2008, *MNRAS*, 383, 557  
 Paumard, T., et al. 2006, *ApJ*, 643, 1011  
 Peres, A. 1962, *Phys. Rev.*, 128, 2471  
 Perets, H. B., & Alexander, T. 2008, *ApJ*, 677, 146  
 Perets, H. B., & Gualandris, A. 2010, *ApJ*, 719, 220  
 Peñarrubia, J., Just, A., & Kroupa, P. 2004, *MNRAS*, 349, 747  
 Peters, P. C., & Mathews, J. 1963, *Phys. Rev.*, 131, 435  
 Ponti, G., Terrier, R., Goldwurm, A., Belanger, G., & Trap, G. 2010, *ApJ*, 714, 732  
 Portegies Zwart, S. F., Baumgardt, H., McMillan, S. L. W., Makino, J., Hut, P., & Ebisuzaki, T. 2006, *ApJ*, 641, 319  
 Prada, F., Klypin, A. A., Cuesta, A. J., Betancort-Rijo, J. E., & Primack, J. 2011, eprint arXiv:1104.5130  
 Preto M., Amaro-Seoane P., 2010, *ApJ*, 708, L42  
 Preto, M., Berentzen, I., Berczik, P., & Spurzem, R. 2011, *ApJ*, 732, L26  
 Quinlan, G. D., & Shapiro, S. L. 1987, *ApJ*, 321, 199  
 Quinlan, G. D. 1996, *New Astronomy*, 1, 35  
 Quinn, P. J. & Goodman, J. 1986, *ApJ*, 309, 472Q  
 Quinn, P. J., Hernquist, L., & Fullagar, D. P. 1993, *ApJ*, 403, 74  
 Rees, M. J. 1988, *Nature*, 333, 523  
 Reid, M. J., & Brunthaler, A. 2004, *ApJ*, 616, 872  
 Ricotti, M. & Gnedin, N. Y. 2005, *ApJ*, 629, 259  
 Ricotti, M., Gnedin, N. Y., & Shull, J. M. 2008, *ApJ*, 685, 21  
 Rownd, B. K. & Young, J. S. 1999, *ApJ*, 118, 670  
 Sánchez-Salcedo, F. J., & Brandenburg, A. 1999, *ApJ*, 522, L35  
 Schödel, R., Merrit, D., & Eckart, A. 2009, *A&A*, 502, 91  
 Sellwood, J. A., Nelson, R. W., & Tremaine, S. 1998, *ApJ*, 506, 590  
 Sesana, A., Haardt, F., & Madau, P. 2007, *MNRAS*, 379, 45  
 Sesana, A., Haardt, F., & Madau, P. 2008, *ApJ*, 686, 432  
 Sesana, A. 2010, *ApJ*, 719, 851  
 Shakura, N. I. & Sunyaev, R. A. 1973, *A&A*, 24, 337  
 Simon, J. D. & Geha, M. 2007, *ApJ*, 670, 313  
 Sinha, M., & Holley-Bockelmann, K. 2012, *ApJ*, 751, 17  
 Snowden, S. L., et al. 1997, *ApJ*, 485, 125  
 Stolte, A., Ghez, A. M., Morris, M., Lu, J. R., Brandner, W., & Matthews, K. 2008, *ApJ*, 675, 1278  
 Strigari, L. E., Bullock, J. S., Kaplinghat, M., Simon, J. D., Geha, M., William, B., & Walker, M. G. 2008, *ApJ*, 454, 1096  
 Su, M., Slatyer, T. R., & Finkbeiner, D. P. 2010, *ApJ*, 724, 1044  
 Šubr, L., Schovancová, J., & Kroupa, P. 2009, *A&A*, 496, 695  
 Stark, A. A., Martin, C. L., Walsh, W. M., Xiao, K., Lane, A. P., & Walker, C. K. 2004, *ApJ*, 614, L41  
 Taylor, J. E. & Babul, A. 2001, *ApJ*, 559, 716  
 Terrier, R., et al. 2010, *ApJ*, 719, 143  
 Tillich, A., Przybilla, N., Scholz, R.-D., & Heber, U. 2009, *A&A*, 507, L37  
 Tormen, G., Bouchet, F. R., & White, S. D. M. 1997, *MNRAS*, 286, 865  
 Toth, G., & Ostriker, J. P. 1992, *ApJ*, 389, 5  
 Velázquez, H. & White, S. D. M. 1999, *MNRAS*, 304, 254  
 Vesperini, E. & Weinberg, M. 2000, *ApJ*, 534, 598  
 Walker, I. R., Mihos, J. C., & Hernquist, L. 1996, *ApJ*, 460, 121  
 Wang, H. Y., Jing, Y. P., Mao, S., & Kang, X. 2005, *MNRAS*, 364, 424  
 Weinberg, M. D. 1997, *ApJ*, 478, 435  
 Wetzel, A. R. 2011, *MNRAS*, 412, 49  
 Widrow, L. M., & Dubinski, J. 2005, *ApJ*, 631, 838  
 Wise, J. H. & Abel, T. 2008, *ApJ*, 684, 1  
 Yelda, S., Lu, J. R., Ghez, A. M., Clarkson, W., Anderson, J., Do, T., & Matthews, K. 2010, *ApJ*, 725, 331  
 Zentner, A. R., Kravtsov, A. V., Gnedin, O. Y., & Klypin, A. A. 2005, *ApJ*, 629, 219  
 Zhao, D. H., Jing, Y. P., Mo, H. J., & Börner, G. 2003, *ApJ*, 597, L9  
 Zubovas, K., King, A. R., & Nayakshin, S. 2011, *MNRAS*, L274